IAEA
International Atomic Energy Agency

INDC(CZR)-0003
Distr. G+J+RD

INDC International Nuclear Data Committee

Validation of ^{nat}Fe and ^{nat}Cr Activation Cross Sections in Quasi-Mono Energetic Neutron Spectra (<35 MeV) Including Irradiation, Measurement and Computational Analysis

Final Report on Task 4.1 of the
Grant Agreement F4E-FPA-395-01
on
"Nuclear Data Experiments and Techniques"

M. Majerle, P. Bém, J. Novák, E. Šimečková, M. Štefánik

Nuclear Physics Institute of ASCR PRI, 250 68 Řež, Czech Republic

October 2016

IAEA Nuclear Data Section, Vienna International Centre, A-1400 Vienna, Austria

Selected INDC documents may be downloaded in electronic form from
http://www-nds.iaea.org/publications/
or sent as an e-mail attachment.
Requests for hardcopy or e-mail transmittal should be directed to
nds.contact-point@iaea.org
or to:

Nuclear Data Section
International Atomic Energy Agency
Vienna International Centre
PO Box 100
A-1400 Vienna
Austria

Produced by the IAEA in Austria
October 2016

INDC (CZR)-0003
Distr. G+J+RD

Validation of ^{nat}Fe and ^{nat}Cr Activation Cross Sections in Quasi-Mono Energetic Neutron Spectra (<35 MeV) Including Irradiation, Measurement and Computational Analysis

Final Report on Task 4.1 of the
Grant Agreement F4E-FPA-395-01
on
"Nuclear Data Experiments and Techniques"

M. Majerle, P. Bém, J. Novák, E. Šimečková, M. Štefánik

Nuclear Physics Institute of ASCR PRI, 250 68 Řež, Czech Republic

October 2016

Abstract

This is the final report for Task-4.1 (Gas production cross section measurement) of FPA-395_01 and discusses the work carried out at NPI Řež. The report presents the neutron spectra measurement by Time-of-flight (TOF) technique for Quasi-mono-energetic (QM) neutron spectra and the results for gas production cross section for natural Fe and Cr. The experimental data are a compared with those available from literature. The computational analysis performed using MCNPX for validating the measured neutron spectra is also addressed.

Table of Contents

Disclaimer

The work leading to this publication has been funded partially by Fusion for Energy under the Grant Agreement F4E-FPA-395-01. This publication reflects the views only of the author, and Fusion for Energy cannot be held responsible for any use which may be made of the information contained therein.

1 Introduction

The gas production due to neutron irradiation presents one of the main concerns for the structural material performance in the future power reactors. Experimental data (cross-sections) above 20 MeV are scarce and estimations of gas production in neutron spectra of future power reactors have large uncertainties. The data on gas production can be obtained either by the direct measurement of the produced charged particles or by the measurement of the radioactive residual nuclei. Data from both approaches are complementary and necessary for a quality cross-section evaluation.

The goal of this work was to validate the evaluated gas production cross-sections in the energy range 20-35 MeV for elements Fe and Cr, two main constituents of the EUROFER steel using the residual measurement method. This was achieved with the irradiation of the target materials with neutrons, subsequent spectroscopy measurements of the produced nuclei and the comparison of the newly measured data with the cross-section evaluations.

The neutron generators at the NPI/Řež provided quasi-monoenergetic neutron spectra in the corresponding energy range. Most of the isotopes produced in (n,charged particle) reactions have rather short decay times (in order of tens of seconds). The pneumatic transport system was developed to quickly transfer the irradiated samples to the spectroscopy laboratory for measurements. The measured reaction rates were validated against the EAF-2010 cross-section database using well known procedures and codes.

This work is the continuation of the program of the measurement and analysis of the neutron cross-sections above 20 MeV, relevant for fusion and accelerator driven facilities. In previous years the activation cross sections were measured for (n,xn) reactions on ^{209}Bi, ^{197}Au, ^{59}Co, and ^{93}Nb.

The details of the present analysis and experimental work were presented and discussed at JEFF-meetings.

2 Main parameters of the NPI/Řež experiments

2.1 Quasi-monoenergetic neutron generator

The experimental facility is described in details in [1], here the main parameters of the arrangement and irradiation are mentioned. Proton beam was directed to a thin Li foil (2 mm, ^{7}Li, 99.9% enrichment) backed with a thick C beam stopper (1 cm) producing quasi-monoenergetic neutrons. The studied samples of natural isotopic mixture of Fe and Cr in the form of thin foils were placed 40 mm from the target front inside a polyethylene transportation container. After the irradiation with the duration of ca. 5 minutes, the container with the sample was pneumatically transported to the spectroscopy laboratory, disassembled and the samples were measured with the HPGe detector. Typical time between the end of the irradiation and the start of the measurement with the HPGe was around 20 seconds. The cycle irradiation-measurement was repeated ca. 4 times for each sample (a new sample was used for each repetition). The pneumatic transport system was then removed and the same materials (together with 0.25-0.5 mm thick foils of Tm, Au, Co, Bi) were irradiated at the distance of 87 mm (Fe) and 88 mm (Cr) for ca. 6 hours to measure longer lived isotopes. Seven irradiations were performed with proton energies 20, 22.5, 25, 27.5, 30, 32.5, and 35 MeV (some results are from previous – pre 2014 - measurements in the position 49 mm from the target front). The FWHM and uncertainty of the incident proton energy were measured to be 1.5% [1]. The time profile of the proton beam was recorded on the second scale with the charge integrator. The isotopes with decay times ranging down to ca. 1 minute were reliably measured and the resulting reaction rates are shown in the Table 1.

The produced neutron spectra were acquired with the NE213 scintillator used in the Time-Of-Flight mode. The distance target-NE213 at different experiments was 3.5-4.5 m. The dynamic threshold technique was used for the NE213 efficiency calculation. Due to the cyclic operation of the U-120M cyclotron and resulting timeframe overlap, the energetic interval of the obtained neutron spectra extends from the maximal neutron energy down to ca. 10 MeV.

The integral number of the produced monoenergetic neutrons was determined through the ^{7}Be activity produced in the Li target, as proposed by Schery [2]. After each irradiation, the lithium foil was measured with the HPGe detector and the amount of the produced ^{7}Be was determined with the spectroscopy accuracy (2-3%). The number of the monoenergetic neutrons in the forward direction was then determined with the formula introduced by Uwamino [3].

2.2 HPGe measurements

Several radioactive products were detected in the Cr and Fe foils by the offline γ-spectroscopy employing two calibrated HPGe detectors with the efficiency around 50% and the energy resolution 1.8-1.9 keV at 1332 keV. The decay γ spectra were measured during the cooling period from tens of seconds up to tens of days. The activities of the specific isotopes at the end of the irradiation were calculated using tabulated decay half-lives and gamma intensities from the ENSDF database [4]. The spectroscopic corrections for the beam instability, cascade coincidences, decay during the irradiation, etc. were taken in account, the activities are calculated at the end of the irradiation time. The uncertainties given in the Tables 1 and 2 include the uncertainty of the gamma peak fitting. The uncertainty of the HPGe detector calibration (ca. 2%) and further systematic uncertainties were discussed in detail in the previous work [5] and are not included in the Tables 1 and 2. In general, the repeatability of the measured reaction rates was determined to be within 10%.

Table 1: Experimental activities in Fe foils measured after the irradiation with the quasi-monoenergetic neutrons from the p+Li reaction. The activities are expressed in [Bq/kg/μC]. The uncertainties shown include only the uncertainties of the gamma peak fitting. The repeatability of the results is within 10%. Some reaction rates at 27.5 MeV are systematically lower than reaction rates at neighbour energies due to the problem with the HPGe detector used in this irradiation, these reaction rates were not used in further analysis.

Proton energy [MeV]/reaction	**20**	**22.5**	**25**	**27.5**	**30**	**32.5**	**35**
^{nat}Fe(n,x)^{57}Mn, 40 mm	5430 ±18%	6420 ±7%	6890 ±5%		8990 ±3%	11300 ±3%	
^{nat}Fe(n,x)^{56}Mn, 87 mm	990 ±2%	1015 ±1%	1098 ±2%	606 ±2%	1440 ±1%	1840 ±1%	2330 ±1%
^{nat}Fe(n,x)^{56}Mn, 40 mm	3630 ±2%	3880 ±2%	4030 ±1%	2680 ±1%	5050 ±4%	7170 ±3%	9480 ±1%
^{nat}Fe(n,x)^{54}Mn, 87 mm	0.168 ±3%	0.162 ±7%	0.178 ±3%	0.357 ±11%	0.77 ±1%	1.38 ±1%	1.99 ±1%
^{nat}Fe(n,x)^{52}Mn, 87 mm			0.013 ±35%	0.127 ±8%	0.712 ±2%	1.59 ±2%	2.38 ±1%
^{nat}Fe(n,x)^{52m}Mn, 87mm						337 ±7%	1120 ±7%
^{nat}Fe(n,x)^{52m}Mn, 40 mm				152 ±20%	331 ±17%	1100 ±5%	2060 ±5%
^{nat}Fe(n,x)^{51Cr}, 87 mm	0.35 ±20%	0.24 ±6%	0.22 ±10%	0.24 ±13%	0.29 ±10%	0.83 ±5%	2.05 ±2%
^{nat}Fe(n,x)^{53}V, 40 mm							510 ±22%
^{nat}Fe(n,x)^{52}V, 40 mm			630 ±7%	1080 ±9%	6250 ±5%	8350 ±6%	10200 ±5%
^{nat}Fe(n,x)^{53}Fe, 40 mm	1500 ±3%	2450 ±2%	3790 ±2%	1960 ±30%	4920 ±3%	4930 ±3%	5700 ±2%
^{nat}Fe(n,x)^{53m}Fe, 40 mm			300 ±10%		460 ±7%	460 ±5%	520 ±8%

^{nat}Fe(n,x)^{52}Fe, 87 mm						0.58 ±8%	1.03 ±4%

Table 2: Experimental activities in Cr foils measured after the irradiation with the neutrons from the p+Be reaction (continuous spectrum). The activities are expressed in [Bq/kg/μC]. The uncertainties shown include only the uncertainties of the gamma peak fitting. The repeatability of the results is within 10%. Some reaction rates at 27.5 MeV are systematically lower than the reaction rates at neighbour energies due to the problem with the HPGe detector used in this irradiation, these reaction rates were not used in further analysis.

Proton energy [MeV]/reaction	**20**	**22.5**	**25**	**27.5**	**30**	**32.5**	**35**	**37.5**
^{nat}Cr(n,x)^{54}V, 40 mm	4450 ±18%	6060 ±27%	4850 ±18%		5180 ±10%	7960 ±10%	9171 ±25%	
^{nat}Cr(n,x)^{53}V, 40 mm	13600 ±5%	18300 ±5%	24100 ±5%	18000 ±7%	33400 ±4%	44400 ±3%	50900 ±10%	
^{nat}Cr(n,x)^{52}V, 40 mm	104E3 ±2%	124E3 ±5%	150E3 ±4%	93E3 ±2%	183E3 ±5%	275E3 ±17%	328E3 ±6%	
^{nat}Cr(n,x)^{48}V, 87 mm			0.0057 ±10%	0.0019 ±10%	0.26 ±10%	0.56 ±7%	1.2 ±10%	1.2 ±3%
^{nat}Cr(n,x)^{48}V, 48 mm							3.34 ±3%	
^{nat}Cr(n,x)^{52}Ti, 40 mm							925 ±18%	
^{nat}Cr(n,x)^{51}Ti, 40 mm	325 ±7%	450 ±5%	790 ±5%	1240 ±40%	2280 ±7%	3080 ±10%	3080 ±12%	
^{nat}Cr(n,x)^{48}Sc, 87 mm			0.79 ±13%	0.19 ±6%	0.99 ±14%	2.3 ±10%	2.7 ±4%	2.8 ±3%
^{nat}Cr(n,x)^{48}Sc, 48 mm							7.8 ±6%	
^{nat}Cr(n,x)^{47}Sc, 87 mm							0.19 ±20%	0.24 ±2%
^{nat}Cr(n,x)^{46}Sc, 87 mm			1.1E-3 ±12%	9.3E-3 ±12%	0.021 ±8%	0.022 ±5%	0.029 ±5%	0.031 ±5%
^{nat}Cr(n,x)^{46}Sc, 48 mm							0.084 ±2%	

^{nat}Cr(n,x)^{51}Cr, 87 mm	16.8 ±1%	23.7 ±1%	31.0 ±1%	39.5 ±1%	42.1 ±1%	39.3 ±1%	42.2 ±1%	45.1 ±1%
^{nat}Cr(n,x)^{51}Cr, 48 mm							128 ±1%	
^{nat}Cr(n,x)^{49}Cr, 87 mm	96 ±5%	194 ±2%	294 ±3%	440 ±2%	455 ±2%	391 ±3%	439 ±2%	468 ±2%
^{nat}Cr(n,x)^{49}Cr, 40 mm	456 ±2%	757 ±1%	1200 ±2%	1570 ±6%	1380 ±2%	1580 ±2%	1580 ±2%	

3 Determination of the neutron spectral shape and the total number of neutrons

The irradiation of the Fe and Cr foils was performed at small target-foil distance. The determination of the neutron spectrum at this position was done in several steps. First the spectrum was measured with the Time-Of-Flight method at the distance 3.5-4.5 m from the target and was used to validate the prediction of the MCNPX simulation. In the second step, MCNPX simulation with necessary corrections was used to obtain the spectrum at the position of the irradiated foils (40, 49 and 87 mm from the target front).

3.1 Time-Of-Flight measurements

At each irradiation, the scintillator ORTEC NE213, size 2”x2”, was placed on the beam axis in the distance ranging from 3.5 m to 4.5 m from the target front. The pulses from the scintillator were recorded simultaneously with the cyclotron radio-frequency (RF) signal with digitizers ZTEC ZT4211 (500MS/s, 8bit) and CAEN V1751 (1000MS/s, 10bit). The ZTEC digitizer recorded the digitized signals to the computer hard disk and the analysis was performed offline, while the CAEN digitizer performed most of the analysis with the onboard FPGA. For each pulse, the time phase related to the RF signal, and the signal surfaces in two time windows (long/short gate) were determined. Good neutron/gamma discrimination was obtained with the charge comparison method. The peak of gammas was used to calibrate the detection system on the time scale (photons travel the distance to the scintillator with the speed of light), and on the amplitude scale (gamma energy is 4.43 MeV as explained below). The neutron signals in the TOF diagram were taken from the maximal amplitude down to 75% of the maximal amplitude for each time bin and divided with the efficiency of the scintillator in the same amplitude range. This procedure is known as the dynamic threshold method and has enabled to separate the neutrons from the first time frame from further neutrons (1 frame corresponds to 40-50 ns, depending of the cyclotron RF). The obtained TOF spectrum was then recalculated to the energy spectrum. The frame overlap allowed to measure the spectrum from the maximal neutron energy down to some 10-15 MeV.

The TOF data from the experiment with 25 MeV protons directed to 2 mm Li target are shown in next figures as an example. The NE213 scintillator was placed 4.45 m from the Li target, cyclotron RF was 22.392MHz. The neutron/gamma discrimination is shown in Figure 1. The gamma photons with the energy of 4.43 MeV originating from the first excited state of the ^{12}C nuclei after the interaction of protons are clearly discriminated from higher energy neutrons. The amplitude of the pulses versus their time phase to the RF signal is plotted in the Fig. 2. The repetitive pattern with the period 44.7 ns (corresponding to cyclotron radio-frequency 22.392MHz) is seen. The peak of 4.43 MeV gammas from the carbon beam stop (placed 1 cm behind the lithium target) has the time width of 2-3 ns, this value determines the time resolution of the measurement. Gammas need 14.8 ns to reach the scintillator which is 4.45 m away, and are used for time calibration (the X-axis is shifted so that the gammas are at 14.8 ns). The neutrons with the energy 23.5 MeV need 68 ns for the same distance. The upper red line correspond to the energy of the neutrons calculated from their time of flight and converted to the electron light output [6], the blue line is the same quantity but shifted back in time for one frame. The pulses registered in the interval between the red lines (lower red line = 0.75 * upper red line) are summed and converted to the energy diagram, which is then divided with the scintillator efficiency calculated with the modified version of the SCINFUL-R code[7], see Fig 3. The resulting energy spectrum after the normalization is shown in the Fig. 4.

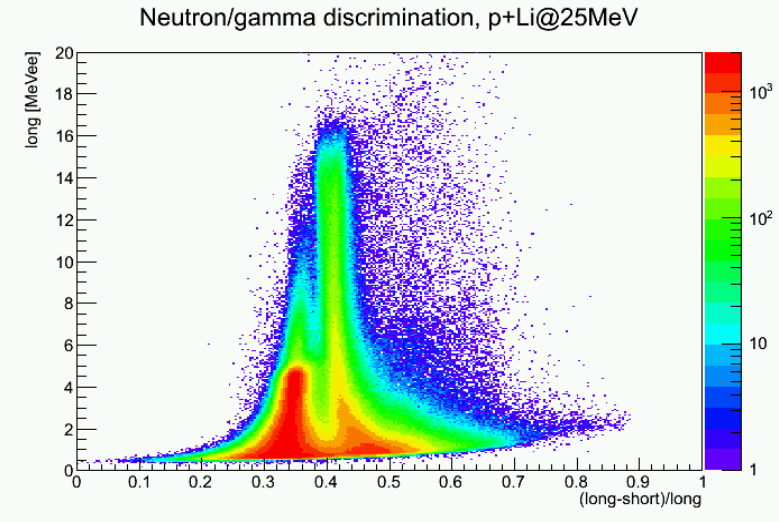

Figure 1 - Neutron/gamma discrimination using the charge comparison method. Gammas with the energy 4.43 MeV (4.13 MeVee) are represented in the left peak. They originate from the excitation of the ^{12}C nuclei with protons (in carbon beam stop). Neutron with energies up to 23.5 MeV (16 MeVee) are represented in the right peak. The labels long and short on the axes are the surfaces under the peaks (summed in two time windows, long corresponds to the amplitude of the signal) recorded with the scintillator detector and normalized to electron light equivalent output units - MeVee.

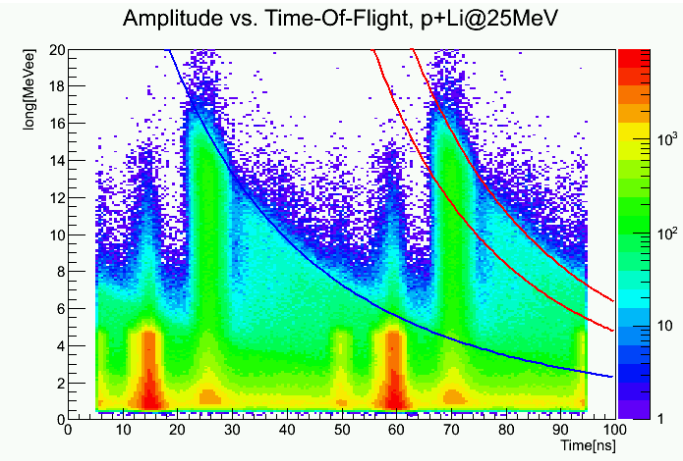

Figure 2 – The amplitude on the pulses distributed in time. The repetitive pattern on the scale 44.7 ns is seen. Two such frames are plotted for better understanding (the first frame is shifted and copied). The pulses were collected during 30 seconds live time with 0.75 μA proton current. Photons need 14.8 ns to travel 4.45 m distance, the neutrons with the energy 23.5 MeV arrive at 68 ns. Red and blue lines mark the energy of neutrons calculated from the time of flight and converted to the electron equivalent light output. The pulses between the two red lines are summed and used in further analysis. The 4.43 MeV photon peak 10 ns before the main peak was identified as the gammas from the proton interaction with the carbon beam collimator placed 80 cm before the Li target.

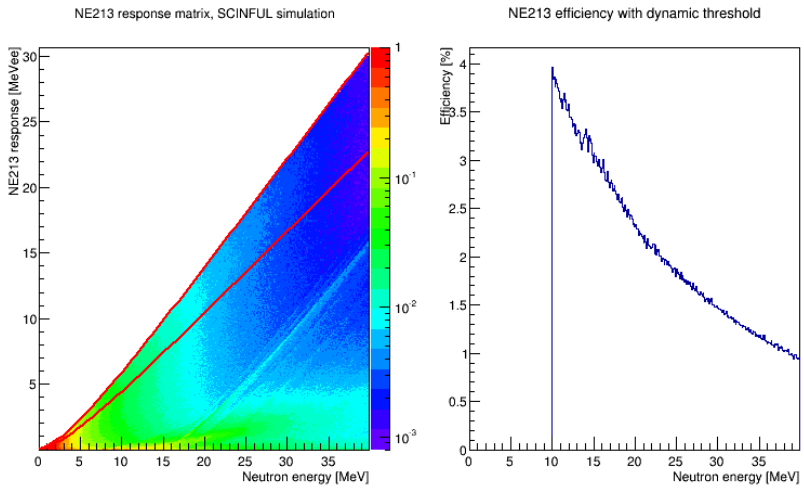

Figure 3 – The efficieny of the 2" x 2" NE213 scintillator was calculated with the modified version of the SCINFUL code. The response of the scintillator to neutron energies in the range 0-40 MeV is on the left side. Two red lines (0.75*max.ampl,max.ampl.) enclose the region used for the efficiency calculation. The efficiency used in further analysis is shown on the right side.

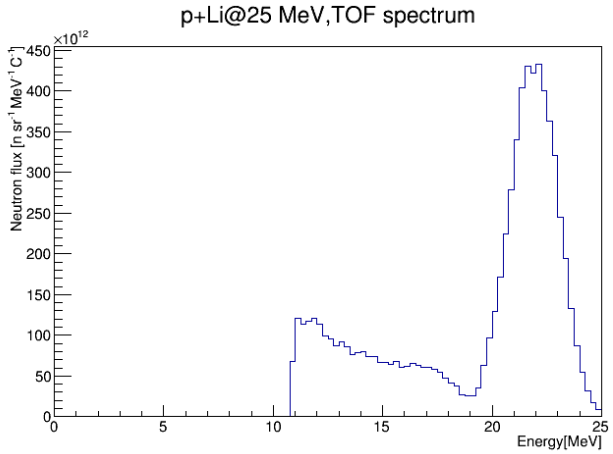

Figure 4 – Neutron energy spectrum calculated from the time of flight measurement.

3.2 MCNPX validation of the measured neutron spectra

The measured neutron spectra were validated with the Monte-Carlo particle transport code MCNPX 2.7.0. The target station was reproduced in the simulation, the realistic distributions of proton energy (Gaussian, FWHM calculated to be 200 keV) and time (Gaussian, FWHM measured to be 2-3 ns) were included. The neutrons were tallied in the volume of the NE213 scintillator for their energy and time of arrival. The spectra measured with the TOF method in this work and the simulated spectra were compared, see Fig. 5. The surface under the monoenergetic peak was normalized for all curves to the produced number of ^{7}Be multiplied with the factor R, as described in the Section 3.3, and only the spectral shapes were compared.

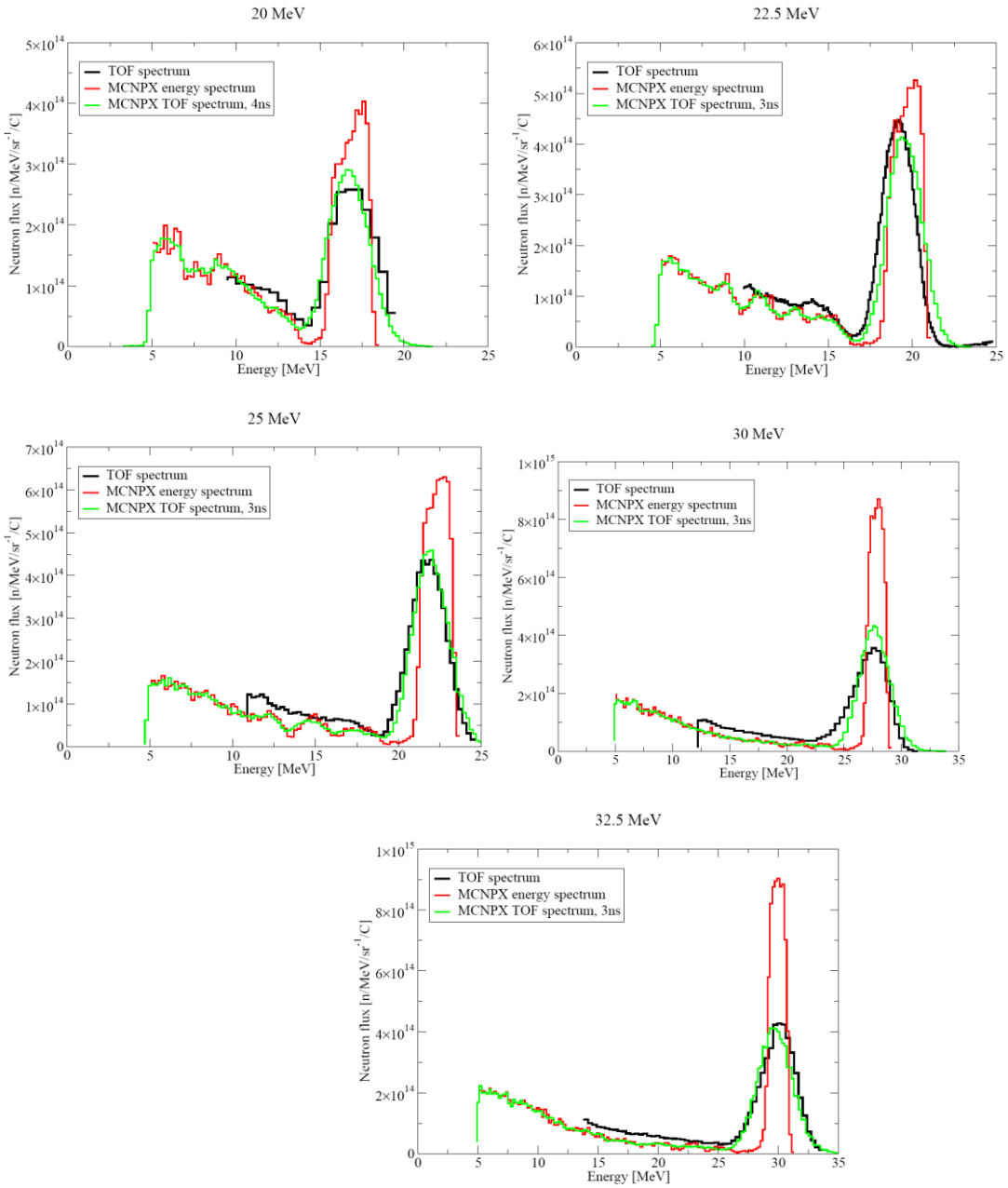

Figure 5 - Experimentally determined Time-Of-Flight spectra and the comparison with the MCNPX simulated spectra. In the simulation, neutron energy and time of arrival were tallied at the distance of the scintillator, the beam was input with realistic energy and time widths (200 keV and 3-4 ns). The number of neutrons in the monoenergetic peak is normalized, see Section 3.3.

The approach with the MCNPX 2.7.0 code was already validated against the TOF data measured by Uwamino at CYRIC [3] in previous F4E work [5]. Both sets of the TOF measurements (Uwamino and this work) can be reproduced well in simulations, and both exhibit a slight underestimation of the neutrons below the monoenergetic peak (for a factor 1.3-1.5).

The neutron spectra which were used for the cross-section calculations were calculated with the MCNPX. The underestimation mentioned above was compensated with the multiplication of the spectrum below the monoenergetic peak for a factor of 1.4. The impact of this multiplication to the final results is discussed in the section dealing with the uncertainties.

3.3 Total number of neutrons, ^{7}Be activity of the irradiated Li target

Schery proposed to obtain the absolute number of the monoenergetic neutrons in the p+Li reaction by the measurement of the ^{7}Be production in Li [2]. The ground and the 0.429 MeV states of the nucleus ^{7}Be (the only two states responsible for the production of the monoenergetic neutrons in the ^{7}Li(p,n)^{7}Be reaction) are the only particle-emission-stable states. The number of the activated ^{7}Be nuclei (which can be accurately measured by the means of the gamma spectrometry) therefore corresponds to the total number of the monoenergetic neutrons emitted to the 4π solid angle.

By measuring the angular dependence of the monoenergetic peak and combining the results of other experimentalists with his own, Uwamino described the ratio of the forward directed monoenergetic neutrons (in respect with the monoenergetic neutrons emitted to the 4π solid angle) with a smooth function (uncertainty 6%) of the proton energy valid in the 20-40 MeV range [3]:

$$R=-5.155\cdot10^{-13}E_p^{4}+4.409\cdot10^{-9}E_p^{3}+2.483\cdot10^{-5}E_p^{2}+6.521\cdot10^{-2}E_p-0.8636.$$

To summarize, from the number of the ^{7}Be activated nuclei in the lithium target and the equation for R, one can determine the number of the forward directed monoenergetic neutrons from the corresponding p+Li reaction. In the time period 2009-present, the number of the produced ^{7}Be nuclei was measured at all experiments with the Li target performed at the NPI Řež. The measured dependency of the ^{7}Be production on the energy of the protons for 2 mm Li is shown in the Figure 6 together with the same measurements performed at CYRIC. Both data sets agree well and were fitted with the second order polynomial function. Schery in his work has measured ^{7}Li(p,n)^{7}Be(0+0.429MeV) reaction cross-sections in the energy range 24.7-44.7 using stacked foil technique, his data recalculated to 2 mm Li are also shown, and are for about 8% larger than our fit.

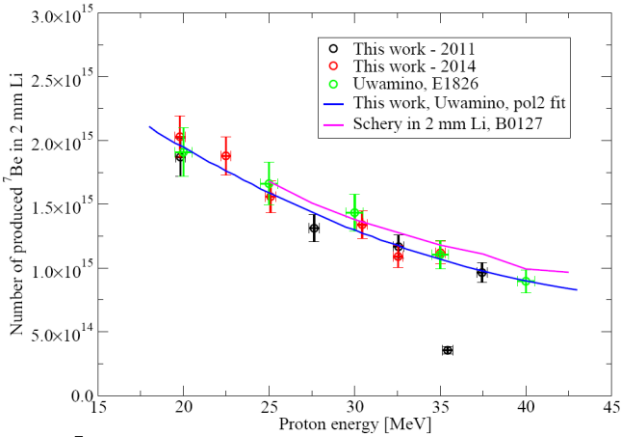

Figure 6 – The production of the ^{7}Be in 2 mm Li irradiated with protons in the energy range 20-40 MeV. Data measured at the NPI Řež and at the CYRIC by Uwamino were fitted with the second order polynomial function. Cross-sections measured by Schery were recalculated to 2 mm Li and are shown for comparison.

3.4 Neutron spectra for NPI/Řež experiments

The neutron spectra were calculated with the MCNPX 2.7.0 code using LA150H and FENDL 3.0 libraries at the place of the irradiated foils. The details of the calculation are described in [5], in this work the additional thin polyethylene transport container was included in the geometry.

The calculated spectra were modified based on the conclusion from the previous sections. First they were normalized so that the number of the neutrons in the monoenergetic peak corresponded to the number of

the produced ^{7}Be in the Li target (described by the blue curve in Fig. 6) multiplied with the factor R. In the second step, the part of the spectrum below the monoenergetic peak was multiplied with a factor 1.4.

4 Extraction of cross-section

4.1 Analysis of existing experimental data on gas production cross-sections in Cr and Fe

The EXFOR database was searched for the existing cross-section data on (n,charged particle) reactions with ^{nat}Fe and ^{nat}Cr cross-section. The published data was obtained either with the direct measurement of the charged particles or with the measurement of the produced residual nuclei using spectrometry methods. These approaches are complementary, eg. measuring charged particles directly does not distinguish between their production modes - (n,p), (n,p+n), .. - on the other hand a measured residual originates from several reactions – (n,α), (n,2p+2n), .. In most cases, one reaction on one isotope dominates and the contributions from other reactions can be subtracted.

The examples of the measured data are shown in the Figure 8. The energy region below 20 MeV is well covered with the measurements, while the data above 20 MeV are rarer. There are also only few measurements of the activation type above 20 MeV (ie. [8], [9], [10]) and only few residuals are measured (partly because of short decay times).

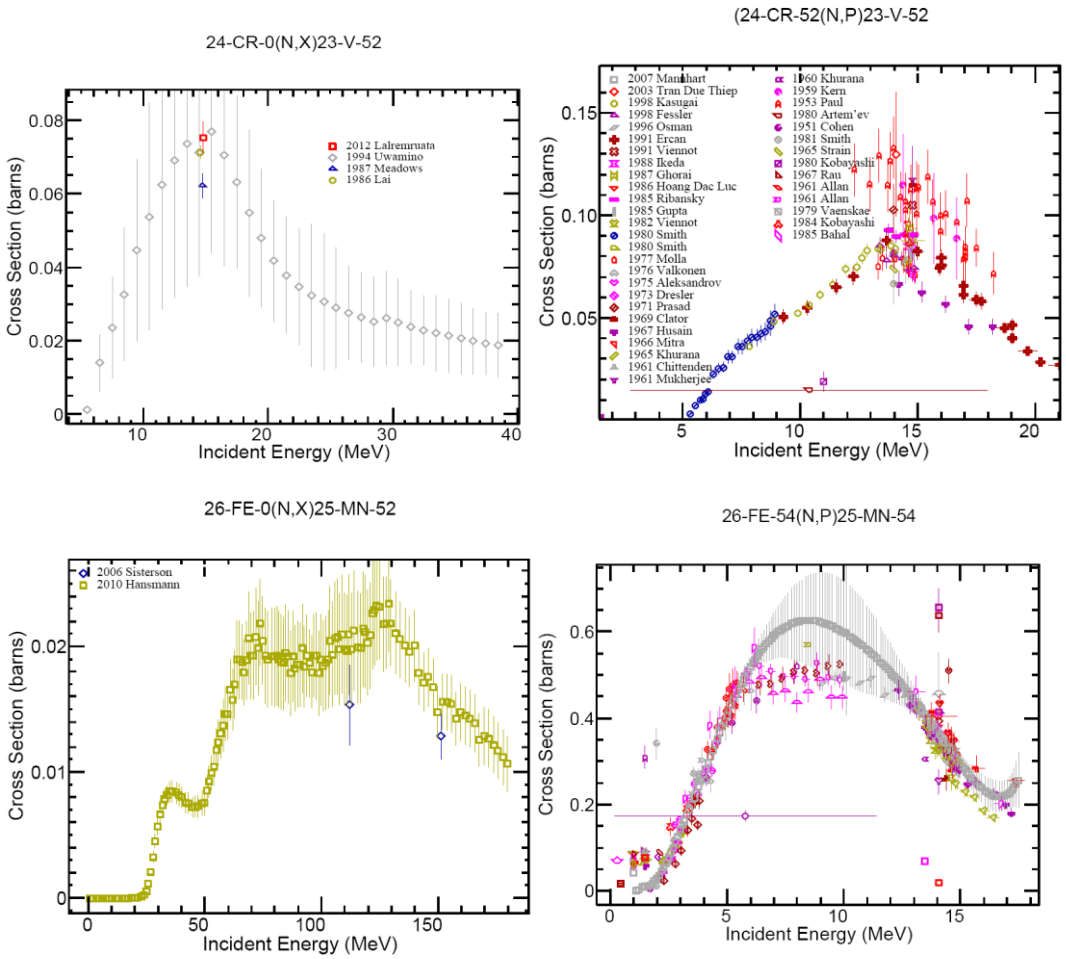

Figure 8 – Examples of the measured data extracted from the EXFOR database. On the left side there are two examples of the residual nuclei measurement – (n,x), on the right side another two examples of the direct measurement of the protons in (n,p) reaction. As can be seen for both examples, only few measurement sets above 20 MeV exist.

4.2 Cross-section extraction procedure

The Li/C source neutron spectra were calculated at the locations of the irradiated samples as described in the Section 3.4. The monoenergetic peak accounts for 30-50% of the total flux, neutrons below the monoenergetic peak origin from the Li breakdown reaction and scattering on the target assembly.

To derive the activation cross-sections curves in such complex neutron field a modified version of the SAND-II [11] code was used, the procedure is described in details in [5].

The EAF-2010 [12,13] evaluated data processed with PREPRO [14] tools and grouped in 0.25 MeV bins were used as the input cross-sections for SAND-II procedure. In the case of contributions of several reactions/isotopes to the produced residual, the according cross-sections were extracted and summed according to the isotope abundance in ^{nat}Fe and ^{nat}Cr, see Fig.9.

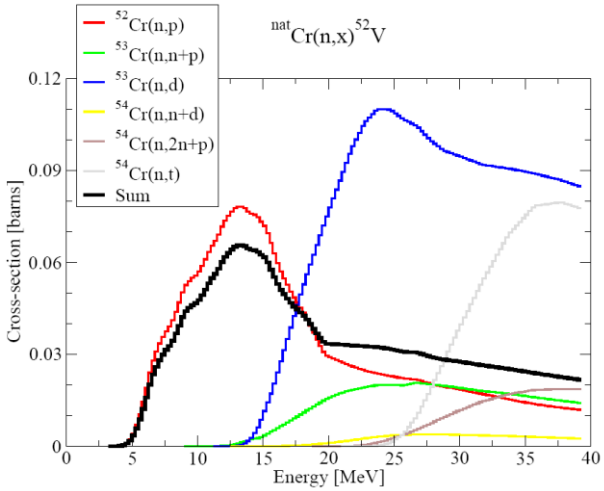

Figure 9 – Cross-sections of all reactions with neutrons on ^{nat}Cr leading to the residual nuclei ^{52}V. The cross-section curves are summed according to the abundance of separate isotopes. In this case, the reaction ^{52}Cr(n,p) is the main contributor to the sum.

The cross-section curve extracted with the SAND-II procedure for the reaction ^{nat}Fe(n,x)^{56}Mn is shown in Figure 10. The curve is obtained after many iterations and does not exhibit physical behaviour. The regions covered with the monoenergetic peaks are clearly seen above 26 MeV (three regions corresponding to irradiations with 30, 32.5 and 35 MeV protons) and below 24 MeV (22.5 and 25 MeV protons). The resulting cross-sections are obtained by averaging the curves in these regions. The broad peak around 25 MeV corresponds to the irradiation at the proton energy 27.5 MeV, where the problems with the HPGe detector were experienced and the corresponding reaction rates were not used in the extraction. The narrow peak around 21 MeV is caused by non-overlapping monoenergetic regions in the neutron spectrum.

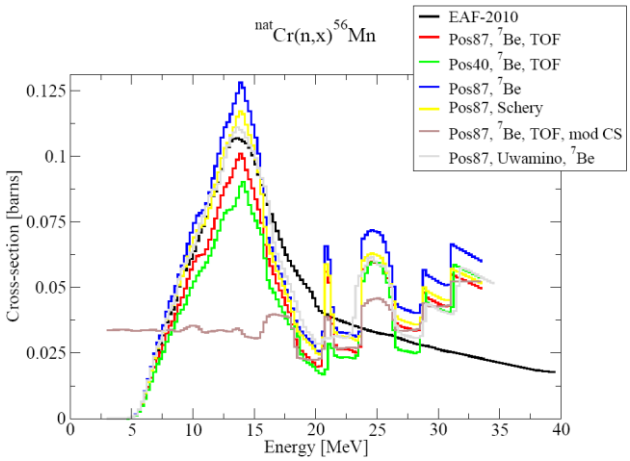

Figure 10 – The comparison of the cross-section curves obtained with the SAND-II extraction procedure. Different input neutron spectra and input cross-section curves were used (see text for details).

The ^{56}Mn isotope decays with the decay constant 2.5785h, and was registered in both short (Pos40) and long (Pos87) term irradiations. The comparison between the extracted curves in the regions corresponding to the monoenergetic peaks shows that the results from both measurements agree up to few percentage points.

Input neutron spectra were varied to study their influence to the results (the regions of the curves corresponding to the monoenergetic peaks). The results marked with "^{7}Be" were obtained with the MCNPX calculated neutron spectra, which were normalized so that the number of the monoenergetic neutrons corresponded to the blue curve from Fig. 6. The "Schery" results were obtained with the spectra normalized to the magenta curve from Fig. 6. The results marked with "^{7}Be, TOF" have the neutron spectra first normalized, then the part of the spectra below the monoenergetic peaks were multiplied with 1.4. The results marked with "Uwamino" were obtained with the neutron spectra interpolated from the TOF measured spectra at CYRIC (procedure is described in [5]) and normalized to the blue curve from Fig. 6. The "^{7}Be" results are systematically higher than "Schery" results, and imply further studies of the ^{7}Li(p,n)^{7}Be reaction cross-sections in the energy range 20-40 MeV. The results obtained with the "Uwamino" input spectra agree well with the results obtained by the neutron spectra determined by the simulations and TOF measurements in this work.

The influence of the input cross-section curve was also studied. The input cross-section curve was set to 1 everywhere above the reaction threshold and 0 below, the default neutron spectra were use in the extraction. In the regions of the monoenergetic peaks the extracted results ("mod CS") are very close to the results of the extraction with the default input cross-section curve and suggest that the results are insensitive to the input cross-section curve.

The final experimental data for the measured cross-sections were obtained from the SAND-II produced curves by taking the average value in the regions determined by the monoenergetic peaks. The uncertainty on the energy scale was set to the width of the peak region (1-2 MeV), the uncertainty on the cross-section scale is mostly defined by the knowledge of the input neutron spectra and is in the range of 10-15% for most cases (see next section).

5 Uncertainty analysis

The detailed analysis of the uncertainties of our cross-section measurements was performed in [5]. The results are summarized in the points below:

- Systematic uncertainty at irradiation (repeatability of the reaction rate measurements) was 10%. The exact number of monoenergetic neutrons was determined from the Li foil thickness (5%) and the proton current measurement (<5%). The impact of the shape of the beam spot, energy FWHM, foil positioning, etc. gives minor contribution to the uncertainty, around few percentage points.
- Uncertainties arose at the cross-section extraction procedure. They were estimated to be 10-15%, and are caused mainly by the uncertain input neutron spectra.
- Systematic uncertainties from the activity measurement (shown with the reaction rates in Tables 1 and 2) are mostly around few percentage points.

In this work, the uncertainties from the first two points were decreased by extra measurements:

- The number of the monoenergetic neutrons was determined from the production of the ^{7}Be in the lithium target and Uwamino formula R (combined accuracy is in order of 5%).
- The spectral shape of the neutron spectra was determined with the TOF measurements.

The effect of these improvements on the combined uncertainty is best seen on the Fig. 10. The differences between the cross-section curves extracted with different input neutron spectra are comparable or below the differences between the results obtained at two irradiation positions (differences between the results obtained with the MCNPX and Uwamino input spectra were generally larger in [5]). This suggests that the main sources of uncertainties from previous work are minimized. The uncertainties arising from the uncertain input cross-section curve are minimal as shown in Fig. 10 and described in [15].

The uncertainties of the final results (10-15%) are defined as quadratic sums of the uncertainties from the spectroscopy part (Tables 1 and 2), and combined uncertainty from the irradiation and extraction part.

6 Final results and comparison to EAF-2010 data

6.1 ^{nat}Fe cross-sections

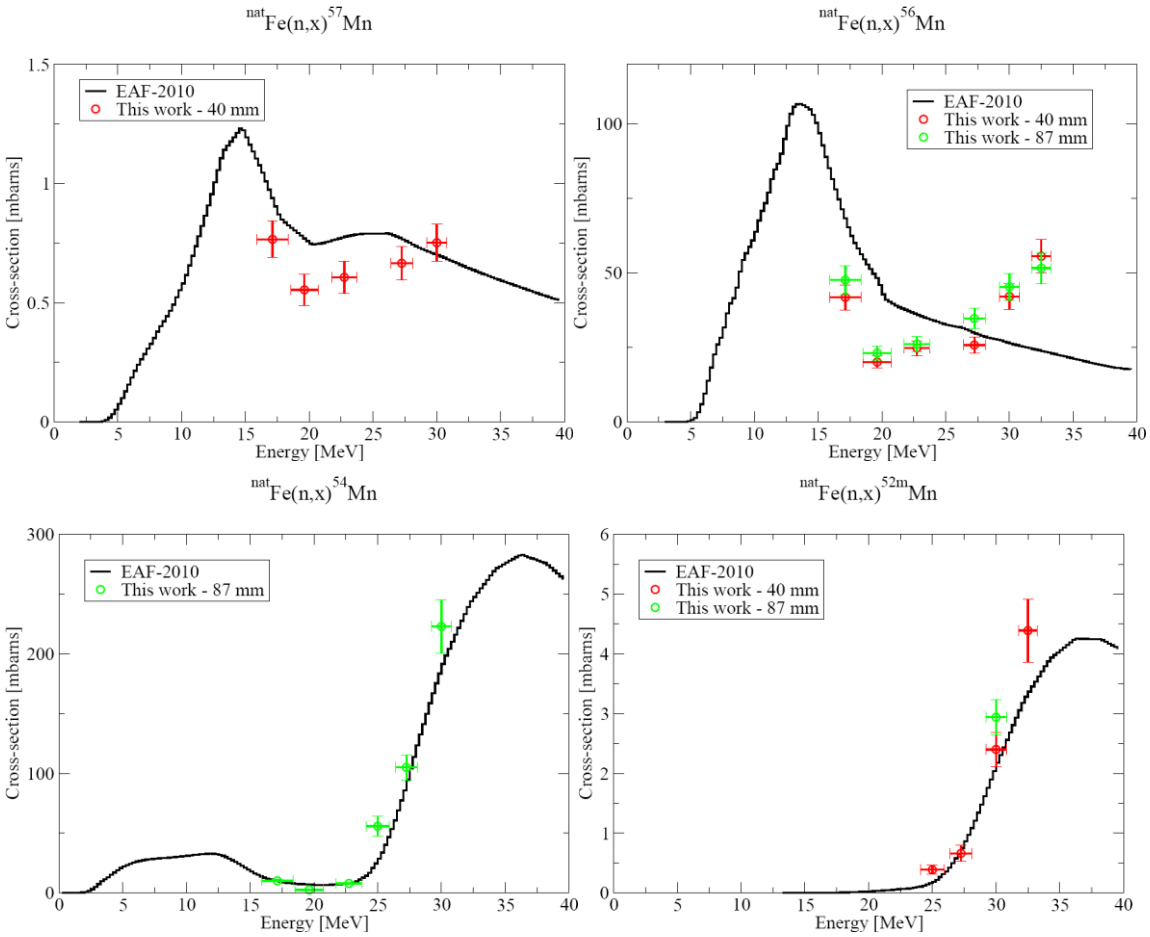

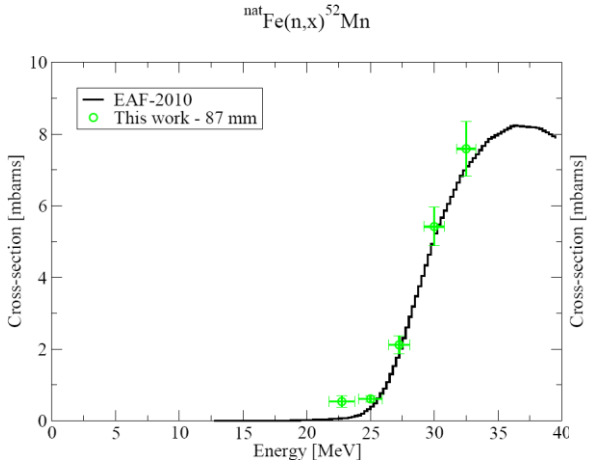
^{nat}Fe(n,x)^{52}Mn
EAF-2010
This work - 87 mm
Cross-section [mbarns]
Energy [MeV]

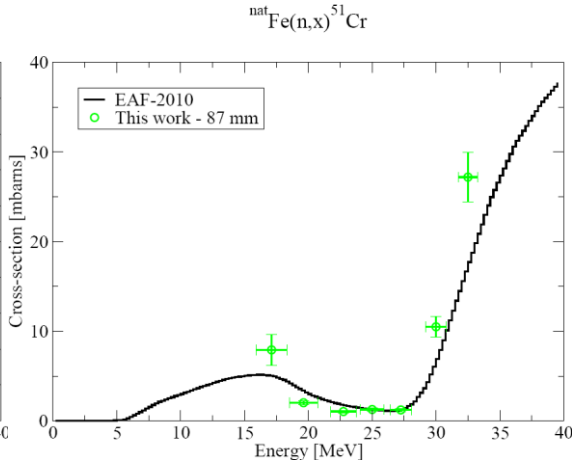
^{nat}Fe(n,x)^{51}Cr
EAF-2010
This work - 87 mm
Cross-section [mbarns]
Energy [MeV]

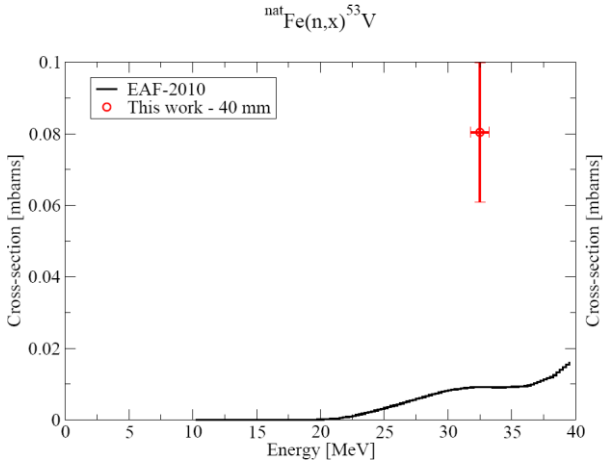
^{nat}Fe(n,x)^{53}V
EAF-2010
This work - 40 mm
Cross-section [mbarns]
Energy [MeV]

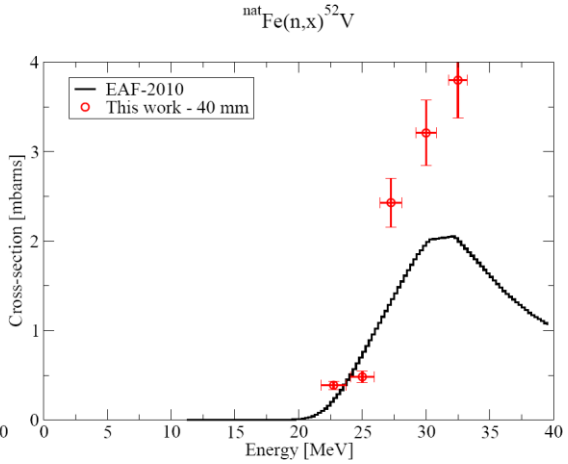
^{nat}Fe(n,x)^{52}V
EAF-2010
This work - 40 mm
Cross-section [mbarns]
Energy [MeV]

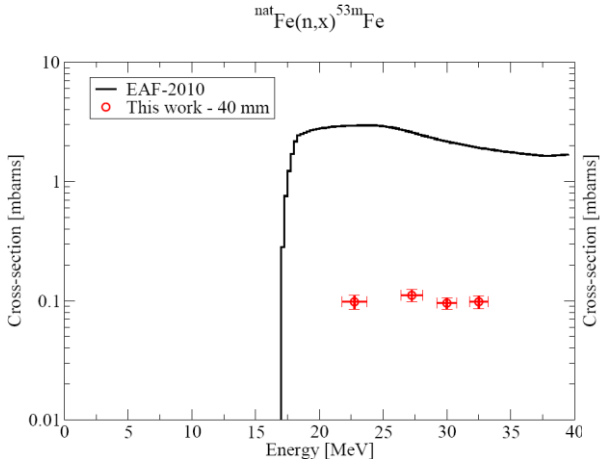
^{nat}Fe(n,x)^{53m}Fe
EAF-2010
This work - 40 mm
Cross-section [mbarns]
Energy [MeV]

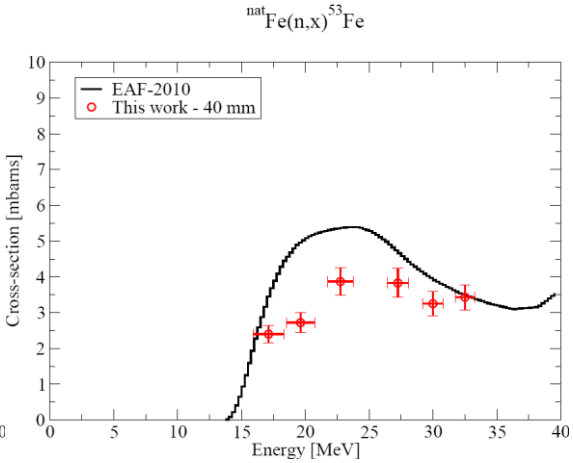
^{nat}Fe(n,x)^{53}Fe
EAF-2010
This work - 40 mm
Cross-section [mbarns]
Energy [MeV]

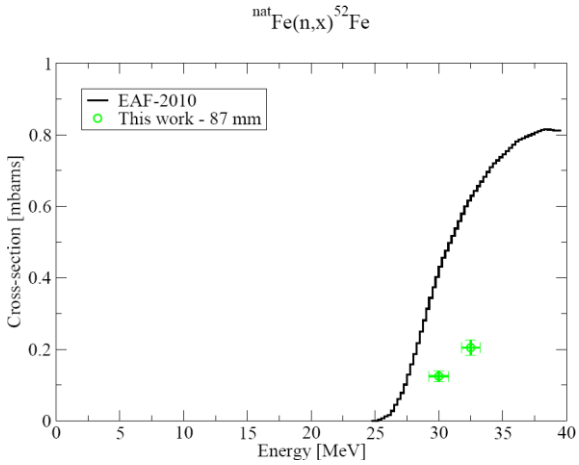

Figure 11 – The cross-sections of ^{nat}Fe(n,x) reactions extracted from the NPI/Řež experimental data with the evaluated data from the EAF-2010 database. The charged particles are produces in the reactions resulting in the residual elements Mn, Cr and V. The (n,xn) reaction cross-sections were also registered (residual element Fe) and are shown for completeness. The red points were obtained with short time irradiation runs (5 min) in the position 40 mm from the Li target front, the blue and the green points were obtained with long time irradiation in the positions 49 mm and 87 mm from the target front. The cross-section curves EAF-2010 were obtained by the sum of all reactions leading to the given residual which are included in the EAF-2010 evaluation.

Most newly measured data points confirm the validity of the EAF-2010 database. In the case of reactions ^{nat}Fe(n,x)^{56}Mn and ^{nat}Fe(n,x)^{57}Mn, the experimental results suggest slightly different shape of the cross-section curve, increasing with the energy – this might be the effect of the another reaction leading to the same isotope, but which is not included in the EAF-2010. As for the reaction ^{nat}Fe(n,x)^{53m}Fe the experimental results indicate that the evaluation significantly overestimates the actual cross-section, on the other hand for the reaction to another isomer state ^{nat}Fe(n,x)^{53}Fe experiment and evaluation agree well. The only reaction contributing to $^{53(g+m)}$Fe production in our energy range is (n,2n) on ^{54}Fe.

6.2 ^{nat}Cr cross-sections

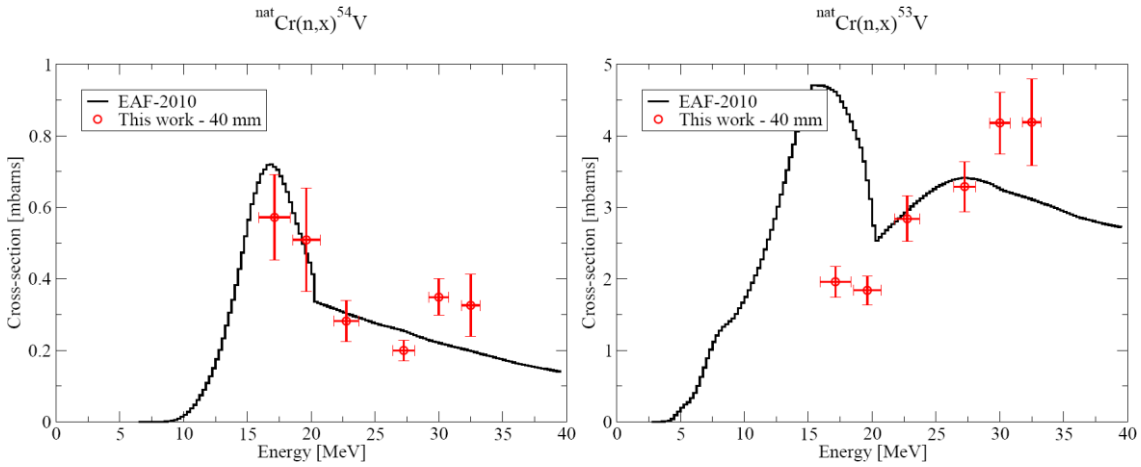

$^{nat}Cr(n,x)^{52}V$

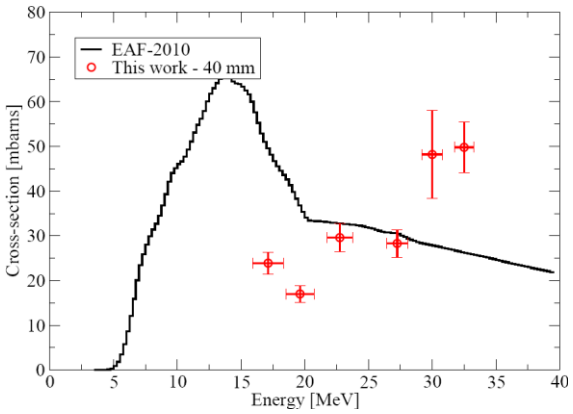

$^{nat}Cr(n,x)^{48}V$

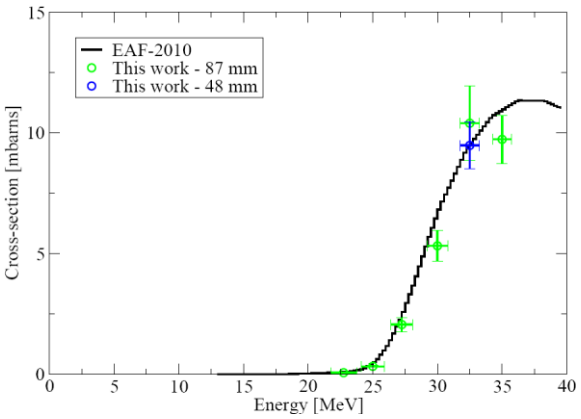

$^{nat}Cr(n,x)^{52}Ti$

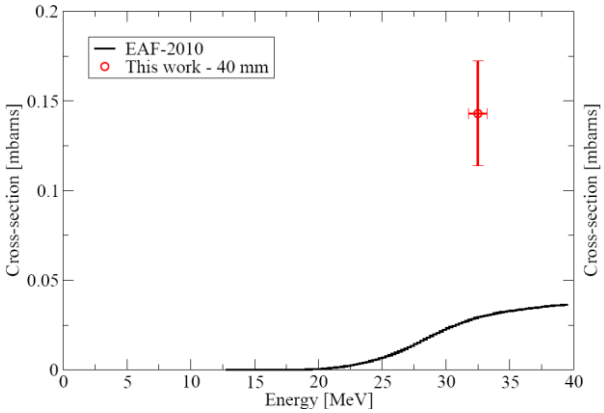

$^{nat}Cr(n,x)^{51}Ti$

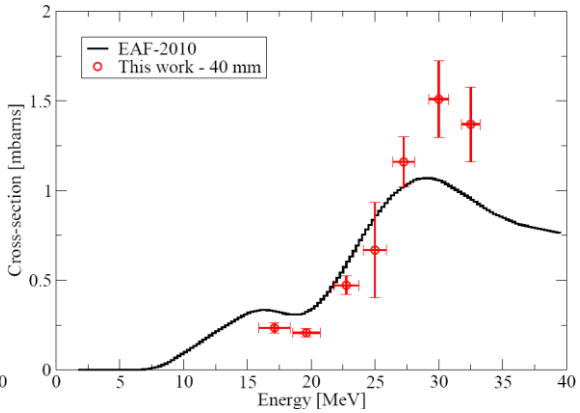

$^{nat}Cr(n,x)^{48}Sc$

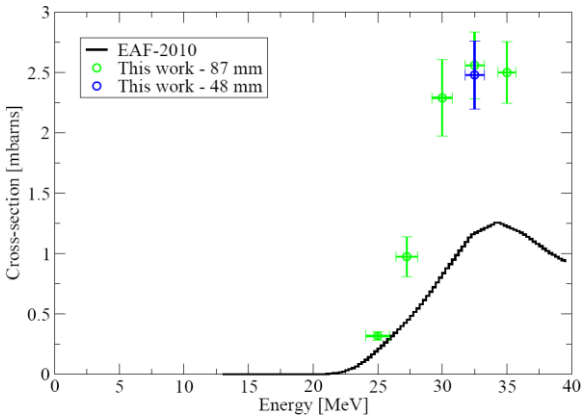

$^{nat}Cr(n,x)^{47}Sc$

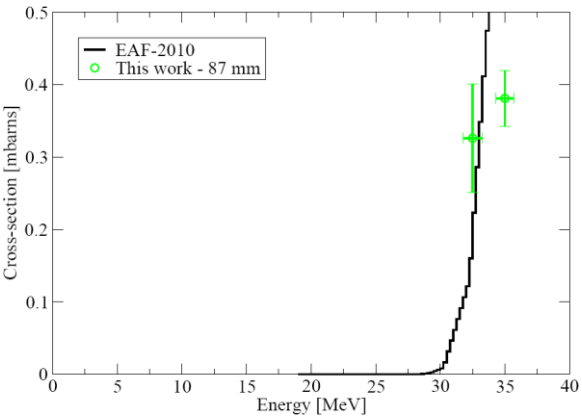

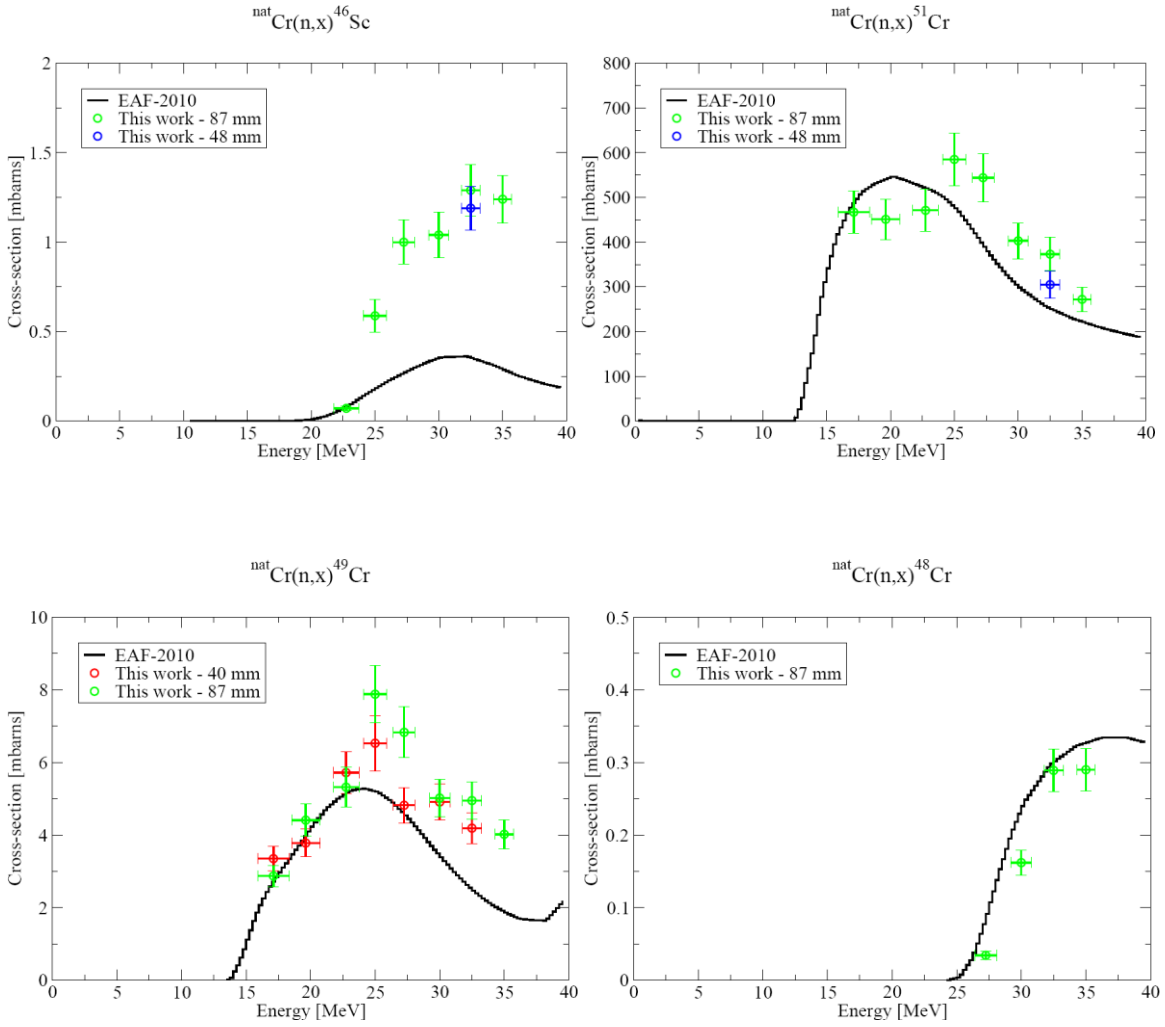

Figure 12 – The cross-sections of ^{nat}Cr(n,x) reactions extracted from the NPI/Řež experimental data with the evaluated data from the EAF-2010 database. The charged particles are produces in the reactions resulting in the residual elements V, Ti, and Sc. The (n,xn) reaction cross-sections were also registered (residual element Cr) and are shown for completeness. The red points were obtained with short time irradiation runs (5 min) in the position 40 mm from the Li target front, the blue and the green points were obtained with long time irradiation in the positions 49 mm and 87 mm from the target front. The cross-section curves EAF-2010 were obtained by the sum of all reactions leading to the given residual which are included in the EAF-2010 evaluation.

Again, the measured data points mostly confirm the validity of the EAF-2010 database. A significant disagreement is observed in the case of the reactions leading to ^{46}Sc and ^{48}Sc. In our energy range, only the reaction (n,p+α) on ^{50}Cr and ^{52}Cr is responsible for these two residuals, which suggest that the EAF-2010 evaluation systematically underestimates the cross-sections of (n,p+α) reactions (this reaction is not present in the production of ^{47}Sc, where good agreement EAF-2010/experiment is found).

7 Conclusion

Task 4.1 was completed successfully. The cross-sections connected with the gas production in ^{nat}Fe and ^{nat}Cr were measured using the residual measurement method and validated with the EAF-2010 database. In regard to previous work, the knowledge of the neutron spectra was improved by new measurements (TOF, ^{7}Be activity), and pneumatic post system was installed to allow the measurement of residuals with shorter decay times (down to tens of seconds). Seven irradiations of ^{nat}Fe and ^{nat}Cr foils were performed with proton energies 20, 22.5, 25, 27.5, 30, 32.5 and 35 MeV, the produced residual nuclei were determined with the gamma-spectrometry. The cross-sections were extracted using the approach with the SAND-II code introduced in previous works [5] and compared with the EAF-2010 evaluated data. Most obtained experimental points connected to gas production confirm the validity of the EAF-2010 database.

References

1) P. Bém, V. Burjan, U. Fischer, M. Götz, M. Honusek, V. Kroha, J. Novák, S.P. Simakov, E. Šimečková, The NPI Cyclotron-based Fast neutron Facility, Int. Conf. on Nuclear Data for Sci. and Techn. (ND-2007), Nice 2007; EDP Sciences 2008, p. 555-558

2) S.D. Schery, et al., Activation and angular distribution measurements of ^{7}Li(p, n)^{7}Be(0.0+0.49 MeV) for E_p=25-45 MeV: A technique for absolute neutron yield determination, NIM 147 (1977) 399-404, EXFOR B0127, doi:10.1016/0029-554X(77)90275-0

3) Y. Uwamino, T.S. Soewarsono et al., High-energy p-Li neutron field for activation experiment, NIM A389 (1997) 463-473, EXFOR E1826, doi:10.1016/S0168-9002(97)00345-8

4) Jag Tuli, NNDC, Brookhaven National Laboratory, Evaluated Nuclear Structure Data File on http://www.nndc.bnl.gov/ensdf/

5) M. Majerle et al., Final Report F4E-2010-GRT-056, Action2, Task 4.2.

6) Saint-Gobain Crystals, BC-501/BC-501A/BC-519 Liquid Scintillators datasheet, http://www.crystals.saint-gobain.com/uploadedFiles/SG-Crystals/Documents/SGC%20BC501_501A_519%20Data%20Sheet.pdf

7) S. Meigo et al., Nucl. Instrum. Meth., A401 (1997) 365-378, doi:10.1016/S0168-9002(97)01061-9

8) D. Hansmann, Dissertation thesis, Fakultät für Mathematik und Physik, Leibniz Universität Hannover, 2010.

9) J.M. Sisterson et al., Nucl. Instrum. Meth., B245 (2006) 371-378, doi:10.1016/j.nimb.2005.12.002

10) Y. Uwamino et al., J. Nucl. Sci. Technol., Vol. 31, Issue 1 (1994) 1-11, doi:10.1080/18811248.1994.9735110

11) SAND-II-SNL Neuron Flux Spectra Determination by Multiple Foil Activation-iterative Method, RSICC Shielding Routine Collection PSR-345, Oak Ridge 1996

12) R.A. Forrest, J. Kopecky, J-Ch. Sublet, The European Activation File: EAF-2007 neutron-induced cross section library, Report UKAEA FUS 535, Culham, 2007

13) J-Ch. Sublet et al., EAF-2010 on http://www.oecd-nea.org/dbforms/data/eva/evatapes/eaf_2010/

14) D.E. Cullen, PREPRO 2010 - 2010 ENDF-6 Pre-processing Codes, Technical report IAEA-NDS-39 (Rev.14), International Atomic Energy Agency, Vienna , Austria

15) M. Majerle et al., Nucl Data Sheets, 111 (2014) 425-428, doi:10.1016/j.nds.2014.08.120

Nuclear Data Section
International Atomic Energy Agency
P.O. Box 100
A-1400 Vienna
Austria

E-mail: nds.contact-point@iaea.org
Fax: (43-1) 26007
Telephone: (43-1) 2600 21725
Web: http://www-nds.iaea.org/